Heredity (2017), 1–7

www.nature.com/hdy

ORIGINAL ARTICLE

# Air-borne genotype by genotype indirect genetic effects are substantial in the filamentous fungus *Aspergillus nidulans*

NO Rode[2], P Soroye, R Kassen and HD Rundle

Genotype by genotype indirect genetic effects (G × G IGEs) occur when the phenotype of an individual is influenced by an interaction between its own genotype and those of neighbour individuals. Little is known regarding the relative importance of G × G IGEs compared with other forms of direct and indirect genetic effects. We quantified the relative importance of IGEs in the filamentous fungus *Aspergillus nidulans*, a species in which IGEs are likely to be important as air-borne social interactions are known to affect growth. We used a collection of distantly related wild isolates, lab strains and a set of closely related mutation accumulation lines to estimate the contribution of direct and indirect genetic effects on mycelium growth rate, a key fitness component. We found that indirect genetic effects were dominated by G × G IGEs that occurred primarily between a focal genotype and its immediate neighbour within a vertical stack, and these accounted for 11% of phenotypic variation. These results indicate that G × G IGEs may be substantial, at least in some systems, and that the evolutionary importance of these interactions may be underappreciated, especially in microbes. We advocate for a wider use of the IGE framework in both applied (for example, choice of varietal mixtures in plant breeding) and evolutionary genetics (kin selection/kin competition studies).
*Heredity* advance online publication, 15 March 2017; doi:10.1038/hdy.2017.9

## INTRODUCTION

In the standard model of quantitative genetics, direct genetic effects (DGEs) represent the contribution of an individual's genes to its phenotype (Fisher, 1918; Lynch and Walsh, 1998), the expression of which is influenced to varying degrees by sources of environmental variance that can include macro- and/or micro-environmental differences in abiotic conditions. However, biotic effects arising from the social environment, including interactions between individuals such as competition, dominance hierarchies or maternal effects, can also contribute to the phenotype of a focal individual. These biotic effects are considered environmental because they are experienced, but not inherited, by the focal individual. The impact on the phenotype of a focal individual attributed to genes in individuals comprising its social environment is known as an indirect genetic effect (IGE, Moore *et al.*, 1997) or associate effect (Griffing, 1967). Because it is individuals in the social environment that generate IGEs, phenotypic evolution can depend upon the composition of the social group. Although the theoretical importance of IGEs on trait evolution has been recognized for some time (see, for example, Moore *et al.*, 1997; Bijma and Wade, 2008), empirical estimates of the nature, magnitude and determining factors of IGEs remain sparse.

To understand the importance of IGEs in governing the outcome of selection, it helps to articulate more precisely how the different sources of genetic effects contribute to phenotypic variance. Both DGEs and IGEs can be partitioned into terms associated with additive and interaction effects. DGEs of an individual's genes can be decomposed into breeding value and interaction effects. The breeding value is the sum of additive genetic effects at different loci, whereas interaction effects represent the contribution of nonadditive genetic effects either among loci (epistasis) or between alleles at the same locus (dominance in diploid organisms). Additive DGEs can be estimated whenever pedigree or kinship relationships are available, whereas 'genotypic' DGEs (where the genotypic value is the sum of additive, epistatic and dominance effects) are typically estimated when only clones or inbred lines are available. IGEs of an individual's genes can be decomposed into a 'social breeding value' and interaction effects. The 'social breeding value' of an individual can be defined as the sum of its additive genetic effects on the phenotype of every other individual in the population (potentially including individuals with the same genotype), whereas interaction effects represent the contribution of nonadditive genetic effects either among loci (epistasis) or between alleles at the same locus (dominance in diploid organisms) on the phenotype of every genotype in a population. Similar to DGEs, additive IGEs are the most commonly investigated component of IGEs when pedigree or kinship relationships are available, whereas 'genotypic' IGEs (that is, the sum of additive, epistatic and dominance effects) are most commonly investigated when clones or inbred lines are available. We will use the generic term 'main IGEs' to refer to either additive IGEs or genotypic IGEs as they affect the phenotype of every other individual similarly, independently of their genotype. In contrast, genotype × genotype IGEs (G × G IGEs, Wolf, 2000) represent another type of IGE whereby the effect of a genotype on another individual's phenotype depends on an interaction between the genotypes of the focal and the interacting individuals. Importantly, G × G IGEs are often nonreciprocal, and hence the effect of genotype

Department of Biology, University of Ottawa, Ottawa, ON, Canada
[2]Current address: INRA, UMR AGAP, Montpellier, France
Correspondence: Dr NO Rode, INRA, UMR AGAP, 2 place Pierre Viala, F-34060 Montpellier, France.
E-mail: nicolas.rode@ens-lyon.org or nicolas.o.rode@gmail.com
Received 2 December 2016; revised 16 January 2017; accepted 17 January 2017

A on the phenotype of genotype B differs from the effect of genotype B on the phenotype of genotype A.

The evolution of any fitness-related traits affected by IGEs will depend on the composition of the population (Bijma and Wade, 2008). As the composition of the population is likely to change as a result of selection, the presence of IGEs is expected to make the fitness landscape more rugged and temporally dynamic (especially in the presence of G×G IGEs, Wolf, 2000). Hence, IGEs can change the rate, magnitude and even direction of evolutionary change (Bijma and Wade, 2008). This has at least two important consequences. First, natural selection on a trait with a negative covariance between DGEs and main IGEs can result in a negative net selective response. Such a response can be observed in plant breeding, where selection for increased yield may result in more intense competition and a decreased yield in subsequent generations (Griffing, 1967). Second, our ability to predict the value of fitness-related traits, and ultimately the outcome of competitive interactions, depends crucially on the relative contribution of DGEs and main IGEs (that result in transitive fitnesses) versus G×G IGEs (that result in nontransitive fitnesses). To see this more clearly, imagine a series of pairwise competitions between $n$ genotypes with fitness as the phenotype of interest. Main IGEs mean that fitness is transitive (that is, if A beats B and B beats C, we can predict that A beats C), whereas G×G IGEs mean that fitnesses may be nontransitive (that is, where A beats B and B beats C, but A does not beat C). Knowledge of such interactions can be especially important in plant breeding when one seeks to identify the combination of varieties that result in the highest yield (Kiær *et al.*, 2009), and in evolutionary ecology, where the aim is to understand the evolution of sexual conflicts (see, for example, Miller and Pitnick, 2002), maternal effects (see, for example, Linksvayer, 2006) or cooperative behaviours (see, for example, Linksvayer, 2007; Buttery *et al.*, 2010).

Although the occurrence of both main and G×G IGEs is not itself controversial, good empirical data on the relative contributions to phenotypic variance of DGE, main IGEs and G×G IGEs are lacking. A quantitative genetic framework is particularly useful for estimating IGEs because it allows us to characterize the genetic basis of social effects, even when the trait mediating the interaction is not known. These models belong to the wider class of quantitative genetic models used to study different forms of genotype by environment interactions (Via, 1993; Figure 1). However, few studies have quantified both main and G × G IGEs and those that have done so used a limited number of genotypes (usually $n<10$) and therefore lack sufficient power to estimate these variance components.

Here we investigate the relative contribution of direct and indirect genetic effects, including G×G IGEs, for a fitness-related trait in a collection of strains of the filamentous fungus, *Aspergillus nidulans*. We use a panel of 41 strains spanning the range of genotypic variation and interactions found in nature (that is, contrasting highly related mutation accumulation lines differing by only one or a few spontaneous mutations, as well as more distantly related wild isolates). The large number of strains in our study markedly improves statistical power for estimating the proportion of phenotypic variance accounted for by main and G×G IGEs. We measure variation in mycelium growth rate (MGR), a trait known to be an important fitness component in both natural and laboratory populations of *A. nidulans* (Pringle and Taylor, 2002) and that positively correlates with other important traits such as spore production in laboratory strains (Schoustra *et al.*, 2009). Previous work in this species indicates that MGR is sensitive to volatile compounds produced by neighbouring colonies and that the reaction to these compounds is genetically determined (Herrero-Garcia *et al.*, 2011; see Ugalde and Rodriguez-Urra, 2014 for a recent review), suggesting that these compounds could represent a proximate cause of IGEs. The precise mechanism behind these neighbour effects on MGR is of secondary concern, however, as our focus is on the relative impact that neighbours have on MGR. More specifically, we aim to quantify the nature and relative importance of G×G interactions on MGR. Our results indicate that IGEs on fungal growth rate are dominated by G×G interactions.

## MATERIALS AND METHODS

### Strains, media and culture conditions

We used a panel of 41 strains comprising 21 wild isolates from Great Britain, 17 mutation accumulation lines and three lab strains used in previous experiments

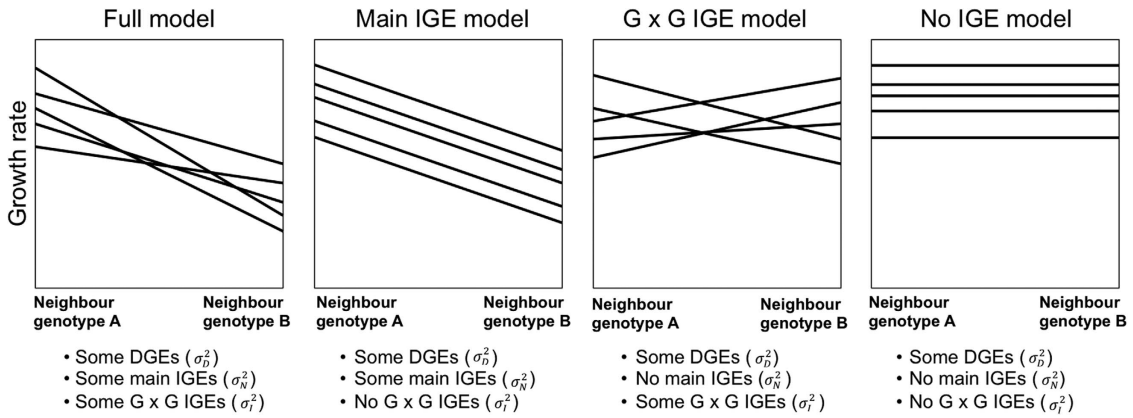


**Figure 1** Graphical representation of the four different models tested, with contrasting relative importance of direct genetic effects (DGEs), main and G×G indirect genetic effects (IGEs). Reaction norms are shown for five focal genotypes grown in two different social environments consisting of neighbour genotype A or B. Lines connect genotypic means in each environment. Main IGEs result in parallel reaction norms to the social environments, whereas G×G IGEs result in nonparallel reaction norms to the social environments. The variance in DGEs, $\sigma_D^2$, is estimated as the average deviation between the overall mean and the mean of each genotype (computed across all social environments). The variance in main IGEs, $\sigma_N^2$, is estimated as the average deviation between the overall mean and the mean of each social environment (computed across all neighbour genotypes). The variance in G×G IGEs, $\sigma_I^2$, is estimated as the average deviation between the mean of each genotype in a given social environment and the mean of this social environment (computed across all neighbour genotypes), after accounting for genotype's mean (computed across all social environments).

(Supplementary Table S1 gives information on these strains). Our culture conditions followed standard protocols for this species (Schoustra *et al.*, 2009). In brief, we produced spore solutions using Complete Medium (CM, set at pH 5.8 and consisting of $NaNO_3$ 6.0 g $l^{-1}$; $KH_2PO_4$ 1.5 g $l^{-1}$; $MgSO_4.7H_2O$ 0.5 g $l^{-1}$; NaCl 0.5 g $l^{-1}$; 0.1 ml of a saturated trace element solution containing $FeSO_4$, $ZnSO_4$, $MnCl_2$ and $CuSO_4$; tryptone 10 g $l^{-1}$; yeast extract 5 g $l^{-1}$; agar 10 g $l^{-1}$ and, added after autoclaving, glucose 4 g $l^{-1}$). We used crossing Minimal Medium (crMM) supplemented with nitrate for the growth assay (crMM recipe identical to CM except for the absence of tryptone and yeast extract, an increased concentration of glucose to 20 g $l^{-1}$ and agar to 30 g $l^{-1}$ and a decreased concentration of $NaNO_3$ to 3 g $l^{-1}$). Such high concentration of agar allows taking fixed area samples using a cork borer and potentially studying traits related to sexual reproduction (for example, cleistothecia density, Kawasaki *et al.*, 2002). Spore suspensions for each strain were prepared by scraping the surface of 3-day-old CM Petri plates (9.5 cm) and washing with 5 ml of a soap solution (distilled water containing NaCl 0.8% and Tween-80 0.0005%). The number of colony-forming units (CFUs) was estimated via serial dilutions and plate counts on CM medium supplemented with Triton X-100 (40 µl $l^{-1}$). The addition of Triton ensures that fungal colonies remain small, facilitating accurate counting. The spore suspension of each strain was diluted to a final concentration of $10^7$ CFUs per ml.

## Experimental design

To facilitate growth rate phenotyping, we focussed on IGEs that occurred between genotypes growing on different plates (that is, 1.5 cm height × 10 cm diameter Petri dishes) physically stacked directly on top of one another. We used a carefully controlled design with 8 replicates for each genotype (16 for JC257), resulting in a total of 336 plates. Plates inoculated with the same strain were randomized in 16 different stacks of 21 plates. With the exception of JC257, no strain was included more than once in a given stack. Although this design prevents a formal test for the presence of genotype by environment interactions (see Discussion), it allows us to directly sum IGE variances of different neighbour genotypes within a stack, thereby greatly simplifying the calculation of IGE variances.

We point inoculated the centre of each crMM plate with approximately the same number of spores using a single 5 µl drop of the $10^7$ CFUs per ml spore suspension. To minimize the effect of condensation, plates were placed upside down within each stack that sometimes resulted in the agar falling onto the lid during the experiment (see statistical analyses below). The occurrence of fallen agar was randomly distributed across genotypes and had no effect on IGEs as the fungus grew through the agar to the opposite side of the point inoculation and then grew normally on the new upper surface of the agar (see Results). Plates were kept in the dark at 37 °C in a large walk-in incubator. Plates were closed but not sealed so that potential air-borne interactions could occur through the airspace below the lid of each plate. We maximized the distance between the different stacks (the minimum distance between two stacks was 60 cm), so that IGEs would be much more likely to occur between genotypes growing on adjacent plates within a stack. After 5 days, all the plates were transferred to a 4 °C refrigerator to prevent further growth. For each plate, colony diameter was measured in two perpendicular directions and the average of these two measurements was used for the analyses.

## Relative importance of main and G×G IGEs

We expect that main IGEs result in parallel reaction norms to the social environments, whereas G×G IGEs result in nonparallel reaction norms to the social environments (Figure 1). We partitioned the phenotypic variance into genetic and environmental components using the ASReml-R package in R (asreml 3.0, VSN International, Hemel Hempstead, UK, Gilmour *et al.*, 2009; R 3.2.0, http://www.r-project.org/, R Development Core Team, 2013). We constructed four different models with contrasting relative importance of DGEs, main IGEs and G×G IGEs (Figures 1 and 2). For the most complex (that is, full) model, we used the following linear mixed model:

$$\boldsymbol{z} = \boldsymbol{Xb} + \boldsymbol{Z_d u_d} + \boldsymbol{Z_n u_n} + \boldsymbol{Z_i u_i} + \boldsymbol{Z_s u_s} + \boldsymbol{\varepsilon} \quad (1)$$

where $\boldsymbol{z}$ is a vector of individual growth rate observations, $\boldsymbol{b}$ is a vector of fixed effects, $\boldsymbol{u_d}$ is a vector of random DGEs, $\boldsymbol{u_n}$ is a vector of random main IGEs, $\boldsymbol{u_i}$ is a vector of random G×G IGEs, $\boldsymbol{u_s}$ is a vector of random stack effects, $\boldsymbol{\varepsilon}$ is a vector of random errors and $\boldsymbol{X}$, $\boldsymbol{Z_d}$, $\boldsymbol{Z_n}$, $\boldsymbol{Z_i}$ and $\boldsymbol{Z_s}$ are incidence matrices relating the observations to the fixed and random effects, respectively (additional details on modelling these genetic effects can be found in Supplementary Methods S1 and Figure S1, and the respective dimensions of $\boldsymbol{u_d}$, $\boldsymbol{u_n}$ and $\boldsymbol{u_i}$ are provided in Supplementary Table S2). Fixed effects in $\boldsymbol{b}$ comprised the overall mean and two variables that accounted for the fallen agar in 22% of the plates. The first controlled for the agar status of the focal plates (factor with two levels: fallen vs not) and the second controlled for the agar status of the plates immediately above and below the focal genotype (continuous variable for the agar fallen in 0, 1 or 2 adjacent plates). The random DGEs and main IGEs in $\boldsymbol{u_d}$ and $\boldsymbol{u_n}$ were assumed to follow a multivariate normal distribution with zero mean vector and variance–covariance matrix:

$$V\begin{bmatrix}\boldsymbol{u_d}\\ \boldsymbol{u_n}\end{bmatrix} = \begin{bmatrix}\sigma_d^2 & \sigma_{dn}\\ \sigma_{dn} & \sigma_n^2\end{bmatrix} \otimes \boldsymbol{I}_{41}$$

where $\boldsymbol{I}_{41}$ represents the identity matrix of dimension equal to the number of genotypes, ⊗ represents the Kronecker product, $\sigma_d^2$ and $\sigma_n^2$ are the variances of DGEs and main IGEs respectively and $\sigma_{dn}$ is the covariance between the mycelium growth of a focal genotype and its main effect as a neighbour (if $\sigma_{dn}<0$, faster growing genotypes inhibit the growth of their neighbours and if $\sigma_{dn}>0$, faster growing genotypes stimulate the growth of their neighbours). The significance of this genetic covariance was tested by including models where it was set to zero. Stack effects account for environmental variation due to different stack positions within the incubator. Random G×G IGEs in $\boldsymbol{u_i}$ and stack effects in $\boldsymbol{u_s}$ were each assumed to be independently and normally distributed with a mean of zero and variance of $\sigma_i^2$ and $\sigma_s^2$ respectively ($V[\boldsymbol{u_i}] = \sigma_i^2\, I_{ni}$ and $V[\boldsymbol{u_s}] = \sigma_s^2\, I_{21}$, Supplementary Table S2). In addition to the full model (equation (1)), we also fit the following three reduced models:

$$\boldsymbol{z} = \boldsymbol{Xb} + \boldsymbol{Z_d u_d} + \boldsymbol{Z_n u_n} + \boldsymbol{Z_s u_s} + \boldsymbol{\varepsilon} \quad \text{(main IGE model)}$$

$$\boldsymbol{z} = \boldsymbol{Xb} + \boldsymbol{Z_d u_d} + \boldsymbol{Z_i u_i} + \boldsymbol{Z_s u_s} + \boldsymbol{\varepsilon} \quad \text{(G× G IGE model)}$$

$$\boldsymbol{z} = \boldsymbol{Xb} + \boldsymbol{Z_d u_d} + \boldsymbol{Z_s u_s} + \boldsymbol{\varepsilon} \quad \text{(No IGE model)}$$

To test the distance over which interactions occurred, we compared a model in which the intensity of IGEs decreased with the inverse of the distance between the plates of neighbour and focal genotypes to a model where IGEs only occurs with genotypes one plate away from the focal genotype (Supplementary Methods S1 and Figure S1). For models with no genetic covariance between DGEs and main IGEs, we also tested for directionality of IGEs (that is, difference in IGEs for a given genotype placed above or below a focal plate) by comparing models where IGEs were similar or different for a

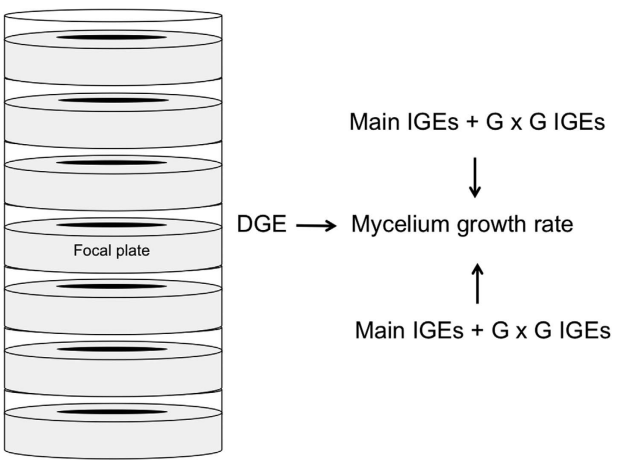


**Figure 2** Schematic representation of the colony diameter of a genotype growing on a focal plate. We used 16 different stacks of 21 plates in the experiment. See text for details regarding estimations of direct and indirect genetic effects.

given genotype placed above or below the focal plate ($V[\boldsymbol{u_i}] = \sigma_I^2\ I_{\text{nI above}}$ and $V[\boldsymbol{u_i}] = \sigma_I^2\ I_{\text{nI below}}$, Supplementary Methods S1 and Supplementary Table S2). We also compared models with and without random stack effects. For the random errors $\boldsymbol{\varepsilon}$, the general form of the variance-covariance matrix was:

$$Var[\boldsymbol{\varepsilon}] = \sigma^2_{\text{cor}}(\Sigma_c \otimes \Sigma_r) + \sigma^2_{\text{uncor}}\boldsymbol{I_n} \quad (2)$$

where $\sigma^2_{\text{cor}}$ and $\sigma^2_{\text{uncor}}$ respectively correspond to spatially correlated and spatially uncorrelated environment variances, $\Sigma_c$ and $\Sigma_r$ represent first-order autocorrelation matrices in the column and row directions respectively (that is, autoregressive models of order one (AR1 models), see Gilmour *et al.*, 2009; Costa e Silva *et al.*, 2013) and where $\boldsymbol{I_n}$ is the identity matrix of dimension equal to the number of observations in the data set. In addition to the usual variance in measurement error ($\sigma^2_{\text{uncor}}$ here), this model accounts for microenvironmental effects within a stack by modelling the shared microenvironment of adjacent plates. Briefly, the correlation between the residuals $\varepsilon_p$ and $\varepsilon_{p+d}$ of two individuals at positions $p$ and $p+d$ within the same stack is modelled as $\text{cor}(\varepsilon_p, \varepsilon_{p+d}) = \rho^{|d|}$. Hence, the further away two individuals are, the lower the correlations between their residuals. We also tested for these spatially correlated and uncorrelated variances by fitting models with only one of these two variance components.

To investigate IGEs occurring between plates up to three positions apart, we discarded data from plates missing neighbour genotypes (that is, when plates were too close to the top or the bottom of the stack), resulting in a data set that included 240 plates (Supplementary Table S3). Both main and G×G IGEs were accurately estimated in our final model: main IGEs were estimated using 41 levels (all genotypes corresponding to these 41 neighbours were replicated at least twice in the data set, Supplementary Table S2) and G×G IGEs were estimated using 417 levels (53 pairs of the 417 pairs were replicated at least twice in the data set, Supplementary Table S2). Importantly, interactions between neighbour genotypes were fitted independently so that G×G IGEs were not assumed to be reciprocal (Supplementary Methods S1). The results were qualitatively similar when modelling IGEs using two larger data sets that included plates that were one and two positions apart, or only one position apart (number of plates = 272 and 304 respectively, Supplementary Tables S4 and S5). Model selection was based on the corrected AICc (Burnham and Anderson, 2002). Models with AICc differences less than two compared with the model with lowest AICc ($\Delta AICc < 2$) were considered as strongly supported by the data, except when they differed from the latter by only one parameter and had essentially the same log-likelihood (Burnham and Anderson, 2002). Fixed effects were also tested using incremental Wald *F*-tests with a 5% significance level (Gilmour *et al.*, 2009). Based on the estimates from the model with lowest AICc, we estimated the proportion of phenotypic variance explained by DGEs (broad sense heritability) and IGEs, and computed their standard errors, using the delta method (Lynch and Walsh, 1998). We included spatially correlated environmental variation in this computation, as we were interested in the proportion of the total phenotypic variance explained and not just genetic and spatially uncorrelated environmental variation. We discuss the relationship between biological IGEs and their statistical interpretation in Supplementary Methods S2. In particular, we show that whenever G×G IGEs depend linearly on the difference in DGEs between focal and neighbour strains, they appear statistically as main IGEs (see Supplementary Methods S2 for details). Finally, we performed simulation-based retrospective power analyses to determine our power to detect G×G IGEs between individual more than one plate apart, $\sigma^2_N$ (variance of main IGEs), and $\sigma_{DN}$ (covariance between the growth of a focal genotype and its main IGE, Supplementary Methods S3).

## RESULTS

### Relative importance of main and G×G IGEs

Results from AICc model selection and Wald *F*-tests on fixed effects are reported in Supplementary Table S3. Estimates from the model with lowest AICc are reported in Supplementary Table S6. The proportion of phenotypic variance in growth explained by among-strain variation in DGE (that is, broad sense heritability) was 81.8% (95% confidence interval (95% CI) = 73.9–89.6%). We found strong evidence for G×G IGEs occurring between plates ($\Delta AIC = 20.3$ for the no IGE model). This indicates that the growth rate of a focal strain depended on an interaction between its genotype and the genotype of each neighbour strain growing one plate above or below it. Overall, these G×G IGEs accounted for 11.4% (95% CI = 6.3–16.6%) of total phenotypic variation.

Models including G×G IGEs with strains more than one plate away from the focal plate had lower support ($\Delta AIC > 2$), suggesting that the interaction between a focal strain and its neighbours occurred over a short spatial scale and became negligible for distances larger than one plate. This conclusion was supported by our power analyses that showed that we were able to detect interactions with genotypes more than one plate away in 97% of our simulations (Supplementary Figure S3). Interestingly, G×G IGEs were largely nondirectional ($\Delta AIC = 4.0$ for a model fitting different G×G IGEs with strains on plates above vs below the focal plate), indicating that a given neighbour strain had the same effect when placed above or below the same focal genotype.

In contrast to G×G IGEs, we did not find strong evidence of main IGEs. The model that included them had low support ($\Delta AICc = 2.1$ compared with the best model) and indicates that main IGEs only explained a small portion of total phenotypic variation (0.7%; 95% CI = 0.0–2.2%). Because of the lack of variation in main IGEs, the model including a covariance between them and DGEs converged with difficulty and also had low support ($\Delta AICc = 4.3$). Our power analyses confirmed that we could detect main IGEs with genotypes one plate away from the focal genotype (when they accounted for more than ~7% of total phenotypic variance, Supplementary Figure S4), and a correlation between DGEs and main IGEs (for genetic correlations higher than 0.1 and values of $\sigma^2_N$ accounting for >5% of total phenotypic variance, Supplementary Figure S5), with at least 80% power. Hence, we found little evidence for the existence of universal stimulator or inhibitor strains (that is, that would affect all genotypes similarly).

We found little support for environmental variation due to stack positions within the incubator (that is, a random stack effect; $\Delta AIC = 2.1$ for a model with this effect). Similarly, the existence of spatially uncorrelated environmental variation (for example, measurement error) had low support ($\Delta AIC = 2.1$ for a model with this effect). In contrast, most of the remaining phenotypic variation was captured by the AR1 error structure (6.8%, 95% CI = 1.9–11.7%; Supplementary Figure S2) with a high autocorrelation coefficient ($\rho = 0.9$, 95% CI = 0.8–1.0), indicating that most of the microenvironmental variation was spatially correlated within a stack (for example, because of different oxygen concentration across positions within a stack). The fall of agar on the lid of the plate slowed the growth of a focal colony, as growth through the fallen agar presumably decreased the measured horizontal growth rate ($\chi^2_1 = 24.3, P = 8.4 \times 10^{-7}$, Supplementary Table S3). In contrast, fallen agar in a neighbour did not affect the growth rate of a focal colony ($\chi^2_1 = 1.0, P < 0.31$, Supplementary Table S3). As plates with fallen agar were randomly distributed across genotypes, the large proportion of G×G IGE observed cannot be explained by this effect.

## DISCUSSION

### Relative importance of main and G×G IGEs

Results from empirical studies suggest that both main and G×G IGEs can account for substantial amounts of phenotypic variation in some taxa (Wolf *et al.*, 2014). Our results provide little support for the existence of main IGEs in *A. nidulans* but strong evidence of G×G IGEs, the latter accounting for ~11% (95% CI = 6.3–16.6%) of phenotypic variation in mycelium growth rate. Our results also

suggest that these interactions occur over relatively short distances (~1 cm), as the support for an interaction between a focal genotype and its neighbour became negligible for distances larger than one plate. Although we could not formally test for genotype by environment interactions (as we did not replicate strains within stacks), pairs of focal and neighbour genotypes were partially replicated at different positions across stacks. It therefore seems unlikely that different replicates of the same pair of focal and neighbour genotypes experienced the same environment, suggesting that genotype by environment interactions are unlikely to have inflated our estimate of the G×G IGE variance. In addition, G×G IGE variances were similar for replicated and unreplicated pairs, suggesting that potential genotype by environment interactions in unreplicated pairs are not a concern (Supplementary Figure S6). Finally, interactions between strains occurred over short distances (~1 cm), and hence interactions between stacks (~60 cm) are unlikely. Hence, we are confident that this large G×G IGE variance between strains within a stack is not a spurious effect of our experimental design.

Main IGEs can account for a substantial portion of phenotypic variation for fitness-related traits (Bergsma *et al.*, 2008; Wolf *et al.*, 2014), and hence our observation that they did not contribute substantial variance for growth rate is striking, though not without precedent (see, for example, Alemu *et al.*, 2014; Nielsen *et al.*, 2014). Our analyses indicate we had sufficient power to detect main IGEs even with small effects (in the range of 10% of total phenotypic variance) and, compared with previous studies that found significant main IGEs, our experimental design had a large number of genotypes and substantial replication. It is therefore unlikely that the absence of main IGEs in our study was because of a lack of power. Rather, we suspect that the apparent absence of main IGEs is a real effect that reflects large variation in the relative importance of G×G IGEs across species and/or traits. For example, species with stronger population structure may exhibit greater G×G IGEs as a result of kin selection. Heterogeneity may also exist across traits, for example, with respect to the strength of their association with fitness (for example, selection will decrease variation in main IGEs faster for traits more closely related to fitness), although this explanation has received little attention. Virtually every study that has tested for G×G IGEs has found them (Wolf *et al.*, 2014), but limited replication in these studies (that typically used $<10$ genotypes) prevents a quantitative comparison of main vs G×G IGEs. Evaluating this idea requires further studies of a range of traits, using a large number of genotypic combinations and a variety of species with contrasting life histories. In addition, accurately accounting for spatially correlated environmental variation can greatly improve IGE estimates. For example, both the magnitude and precision of our G×G IGE estimate were reduced in a model that excluded this variation (8.9%; 95% CI = 0.0–18.7%).

### Potential mechanisms for G×G IGEs on growth rate

The IGEs we detected could be due to a modification of local environmental parameters (for example, humidity or oxygen) and/or to the production of allelochemicals (that is, volatile organic compounds acting as pheromones, Calvo *et al.*, 1999, 2001). In the past decade, a number of studies in the *Aspergillus* genus have shown that compounds such as oxylipins can be used for long-distance interactions both at the interspecific (for example, in fungus–fungus, Roze *et al.*, 2007; fungus–plant, Brodhagen *et al.*, 2008; or fungus bacterium interactions, Spraker *et al.*, 2014) and intraspecific levels (Roze *et al.*, 2010; Herrero-Garcia *et al.*, 2011; see Ugalde and Rodriguez-Urra, 2014 for a review). Importantly, even if a single compound is involved in these G×G IGEs on growth rate, the underlying metabolic pathway could be determined by a large number of loci.

In theory, the amount of signalling molecule emitted by a genotype could be directly proportional to its phenotypic or genotypic value for growth rate. This does not seem to be an appropriate explanation for our results, however, for two reasons. First, the growth rate of a focal genotype was not affected by the agar falling on the plate of a neighbour genotype. Second, IGEs that depend on the growth rate of a genotype would likely translate into main IGEs (see Supplementary Methods S2) that we did not detect here. Hence, our result suggests that there is no signal emitted by an individual colony that would affect every other colony similarly. In particular, the signal emitted by a colony seems to be independent from its diameter. The molecular mechanisms controlling the development of *A. nidulans* are well understood and could help in determining the proximate mechanisms responsible for these interactions. Such a study could also shed light on whether the same loci are involved in signal emission and reception (that is, to explore the extent of pleiotropy of G×G IGEs on growth rate).

### Contact-independent vs contact-dependent IGEs

Our experiment focussed on contact-independent interactions but IGEs may also result from direct physical contact when genotypes are grown together. Allowing physical interactions could affect the relative importance of main vs G×G IGEs, as well as the correlation between DGEs and main IGEs (for example, through competition for resources, Costa e Silva *et al.*, 2013). Using fluorescent markers such as cell trackers or genetic markers would be a powerful alternative to perform competition experiments allowing for direct physical interactions (see, for example, Buttery *et al.*, 2010). However, the direct effect of the marker on the trait of interest (as well as its epistatic effect with the genetic background of the focal and neighbour strains) would need to be carefully accounted for. For example, performing the same competition with different markers might help in estimating main and G×G IGEs while accounting for marker effects. The increased number of competitive combinations necessary to separate these effects might tradeoff with the number of genotypes used for the competition experiments, and the end result might be a decrease in the power to estimate main and G×G IGEs. Pool sequencing using next-generation sequencing technologies could offer a promising alternative to estimate the proportion of each genotype in competition. Further studies in microbes and other species will be important to shed more lights on contact-dependent and contact-independent interactions that shape main and G×G IGEs.

### Use of G×G IGEs in plant breeding

Recent studies have shown that increasing the diversity of cropping systems could be used to develop a sustainable, low-input agriculture (see, for example, Litrico and Violle, 2015). Indeed, selecting mixtures of different plant varieties or species rather than pure stands can increase plant productivity (Kiær *et al.*, 2009) or improve pest and disease management, pollination services or soil processes (Hajjar *et al.*, 2008). By accounting for the interactions between individuals, the IGE quantitative genetic framework provides a means of selecting for one or several traits in a mixture of genotypes (or species) and extends classical selection schemes based on general and specific combining abilities (Sprague and Tatum, 1942). If different species are combined, this framework can be used to increase yield within each species while selecting for positive interactions (or equivalently selecting against negative interactions) between species. Similarly, if different inbred lines are combined, G×G IGEs can be used to choose

the combination of genotypes providing the highest yield. As opposed to other selection schemes that involve selecting genotypes separately (see, for example, Litrico and Violle, 2015), a scheme based on main and G×G IGEs does not require *a priori* knowledge of the traits mediating the interaction between genotypes. In addition, as demonstrated by this study, AR1 models can accurately control for environmental heterogeneity (Gilmour *et al.*, 2009) and improve the efficacy of artificial selection (Costa e Silva *et al.*, 2013).

### G×G IGEs and relatedness

Differences in the phenotype of a focal individual when interacting with kin or non-kin individuals can represent a G×G IGE. IGE quantitative genetics represent a powerful framework for dissecting the effects of relatedness on fitness, as it makes it possible to simultaneously control for differences in average fitness among genotypes and in competitive ability among neighbour genotypes (a common confounding effect in kin selection studies, File *et al.*, 2012). We are aware of only two studies that investigated the effect of relatedness on fitness-related traits using an IGE framework (Alemu *et al.*, 2016; Khaw *et al.*, 2016). The first showed no differences in genetic interactions between kin and non-kin mink (Alemu *et al.*, 2016), whereas the second showed differences in genetic interactions between kin and non-kin tilapia, although genotype by environment interactions could not be ruled out as an alternative explanation (Khaw *et al.*, 2016). Both studies have focussed on the effect of relatedness on trait variance. To our knowledge, most studies that investigated the effect of relatedness on trait mean (using either discrete, for example, Masclaux *et al.*, 2010, or continuous, for example, Stachowicz *et al.*, 2013, measures of relatedness) did not use the IGE framework. Although our experimental design would allow us to test for an effect of relatedness on growth rate, we lacked accurate information on the genetic distance between our strains. We foresee increasing use of the IGE framework in kin selection/competition studies in the future.

In conclusion, we found little support for the existence of main IGEs and strong support for the existence of substantial G×G IGEs, accounting for 11% of phenotypic variation in growth rate. Hence, the importance of air-borne social interactions on fitness-related traits such as growth rate might have been underappreciated in fungi. We advocate a wider use of the IGE framework in applied genetics and in kin selection/competition studies.

## DATA ARCHIVING

Data and scripts used for the analyses are available from Dryad Digital Repository (http://dx.doi.org/10.5061/dryad.hg600).

## CONFLICT OF INTEREST

The authors declare no conflict of interest.

## ACKNOWLEDGEMENTS

We thank Marijke Slakhorst, Fons Debets, Arjan de Visser and Sijmen Schoustra for providing the mutation accumulation lines. We are grateful to Jarrold Hadfield, Arthur Gilmour and Laurène Gay for insightful suggestions regarding statistical analyses in ASReml. We also thank Michael Statsny for helping with growth rate measurements and Florence Débarre for useful comments on an early draft of this manuscript. This work was supported by the Natural Sciences and Engineering Research Council of Canada (to HDR and RK) and the Bettencourt Schueller Foundation, the Agence National de la Recherche (ANR SEAD) and the Marie Skłodowska-Curie/AgreenSkills Program (to NOR).

## AUTHOR CONTRIBUTIONS

NOR designed the experiment and wrote the manuscript together with HDR and RK. NOR and PS carried out the experiment. NOR performed the statistical analyses. All authors discussed the results, read and approved the final manuscript.

Alemu SW, Berg P, Janss L, Bijma P (2016). Estimation of indirect genetic effects in group-housed mink (Neovison vison) should account for systematic interactions either due to kin or sex. *J Anim Breed Genet* **133**: 43–50.

Alemu S, Bijma P, Møller S, Janss L, Berg P (2014). Indirect genetic effects contribute substantially to heritable variation in aggression-related traits in group-housed mink (Neovison vison). *Genet Sel Evol* **46**: 30.

Bergsma R, Kanis E, Knol EF, Bijma P (2008). The contribution of social effects to heritable variation in finishing traits of domestic pigs (*Sus scrofa*). *Genetics* **178**: 1559–1570.

Bijma P, Wade MJ (2008). The joint effects of kin, multilevel selection and indirect genetic effects on response to genetic selection. *J Evol Biol* **21**: 1175–1188.

Brodhagen M, Tsitsigiannis DI, Hornung E, Goebel C, Feussner I, Keller NP (2008). Reciprocal oxylipin-mediated cross-talk in the *Aspergillus*-seed pathosystem. *Mol Microbiol* **67**: 378–391.

Burnham KP, Anderson DR (2002). *Model Selection and Multimodel Inference: A Practical Information-Theoretic Approach*. Springer Science & Business Media: New York, NY, USA.

Buttery NJ, Thompson CRL, Wolf JB (2010). Complex genotype interactions influence social fitness during the developmental phase of the social amoeba *Dictyostelium discoideum*. *J Evol Biol* **23**: 1664–1671.

Calvo AM, Gardner HW, Keller NP (2001). Genetic connection between fatty acid metabolism and sporulation in *Aspergillus nidulans*. *J Biol Chem* **276**: 25766–25774.

Calvo AM, Hinze LL, Gardner HW, Keller NP (1999). Sporogenic effect of polyunsaturated fatty acids on development of *Aspergillus* spp. *Appl Environ Microbiol* **65**: 3668–3673.

Costa e Silva J, Potts BM, Bijma P, Kerr RJ, Pilbeam DJ (2013). Genetic control of interactions among individuals: contrasting outcomes of indirect genetic effects arising from neighbour disease infection and competition in a forest tree. *New Phytol* **197**: 631–641.

File AL, Murphy GP, Dudley SA (2012). Fitness consequences of plants growing with siblings: reconciling kin selection, niche partitioning and competitive ability. *Proc R Soc B Biol Sci* **279**: 209–218.

Fisher RA (1918). The correlation between relatives on the supposition of Mendelian inheritance. *Trans R Soc Edinburgh* **52**: 399–433.

Gilmour AR, Gogel BJ, Cullis BR, Thompson R, Butler D (2009). ASReml user guide release 3.0. VSN International Ltd.: Hemel Hempsted, UK. Available at: https://www.vsni.co.uk/downloads/asreml/release3/UserGuide.pdf.

Griffing B (1967). Selection in reference to biological groups I. Individual and group selection applied to populations of unordered groups. *Aust J Biol Sci* **20**: 127–140.

Hajjar R, Jarvis DI, Gemmill-Herren B (2008). The utility of crop genetic diversity in maintaining ecosystem services. *Agric Ecosyst Environ* **123**: 261–270.

Herrero-Garcia E, Garzia A, Cordobés S, Espeso EA, Ugalde U (2011). 8-Carbon oxylipins inhibit germination and growth, and stimulate aerial conidiation in *Aspergillus nidulans*. *Fungal Biol* **115**: 393–400.

Kawasaki L, Sánchez O, Shiozaki K, Aguirre J (2002). SakA MAP kinase is involved in stress signal transduction, sexual development and spore viability in Aspergillus nidulans. *Mol Microbiol* **45**: 1153–1163.

Khaw HL, Ponzoni RW, Yee HY, bin Aziz MA, Bijma P (2016). Genetic and non-genetic indirect effects for harvest weight in the GIFT strain of Nile tilapia (Oreochromis niloticus). *Aquaculture* **450**: 154–161.

Kiær LP, Skovgaard IM, Østergård H (2009). Grain yield increase in cereal variety mixtures: a meta-analysis of field trials. *F Crop Res* **114**: 361–373.

Linksvayer TA (2006). Direct, maternal, and sibsocial genetic effects on individual and colony traits in an ant. *Evolution* **60**: 2552–2561.

Linksvayer TA (2007). Ant species differences determined by epistasis between brood and worker genomes. *PLoS One* **2**: e994.

Litrico I, Violle C (2015). Diversity in plant breeding: a new conceptual framework. *Trends Plant Sci* **20**: 604–613.

Lynch M, Walsh B (1998). *Genetics and Analysis of Quantitative Traits*. Sinauer: Sunderland, MA, USA.

Masclaux F, Hammond RL, Meunier J, Gouhier-Darimont C, Keller L, Philippe R (2010). Competitive ability not kinship affects growth of *Arabidopsis thaliana* accessions. *New Phytol* **185**: 322–331.

Miller GT, Pitnick S (2002). Sperm-female coevolution in *Drosophila*. *Science* **298**: 1230–1233.

Moore AJ, Brodie ED III, Wolf JB (1997). Interacting phenotypes and the evolutionary process: I. Direct and indirect genetic effects of social interactions. *Evolution (NY)* **51**: 1352–1362.

Nielsen HM, Monsen BB, Ødegård J, Bijma P, Damsgård B, Toften H *et al.* (2014). Direct and social genetic parameters for growth and fin damage traits in Atlantic cod (Gadus morhua). *Genet Sel Evol* **46**: 5.

Pringle A, Taylor J (2002). The fitness of filamentous fungi. *Trends Microbiol* **10**: 474–481.

R Development Core Team (2013). R: A Language and Environment for Statistical ComputingR Foundation for Statistical Computing: Vienna, Austria.

Roze LV, Beaudry RM, Arthur AE, Calvo AM, Linz JE (2007). Aspergillus volatiles regulate aflatoxin synthesis and asexual sporulation in *Aspergillus parasiticus*. *Appl Environ Microbiol* **73**: 7268–7276.

Roze LV, Chanda A, Laivenieks M, Beaudry RM, Artymovich KA, Koptina AV *et al*. (2010). Volatile profiling reveals intracellular metabolic changes in *Aspergillus parasiticus*: veA regulates branched chain amino acid and ethanol metabolism. *BMC Biochem* **11**: 33.

Schoustra SE, Bataillon T, Gifford DR, Kassen R (2009). The properties of adaptive walks in evolving populations of fungus. *PLoS Biol* **7**: e1000250.

Sprague GF, Tatum LA (1942). General vs. specific combining ability in single crosses of corn. *Agron J* **34**: 923–932.

Spraker JE, Jewell K, Roze LV, Scherf J, Ndagano D, Beaudry R *et al*. (2014). A volatile relationship: profiling an inter-kingdom dialogue between two plant pathogens, *Ralstonia solanacearum* and *Aspergillus flavus*. *J Chem Ecol* **40**: 502–513.

Stachowicz JJ, Kamel SJ, Hughes AR, Grosberg RK (2013). Genetic relatedness influences plant biomass accumulation in eelgrass (Zostera marina). *Am Nat* **181**: 715–724.

Ugalde U, Rodriguez-Urra AB (2014). The Mycelium Blueprint: insights into the cues that shape the filamentous fungal colony. *Appl Microbiol Biotechnol* **98**: 8809–8819.

Via S (1993). Adaptive phenotypic plasticity: target or by-product of selection in a variable environment? *Am Nat* **142**: 352–365.

Wolf JB (2000). Indirect genetic effects and gene interactions. In: Wolf JB, Brodie III ED, Wade MJ (eds), *Epistasis and the Evolutionary Process*. Oxford University Press: Oxford, UK, pp 158–176.

Wolf JB, Royle NJ, Hunt J (2014). Genotype-by-environment interactions when the social environment contains genes. In: Hunt J, Hosken D (eds), *Genotype-by-Environment Interactions and Sexual Selection*. John Wiley & Sons, Ltd: Chichester, UK, pp 63–97.

Supplementary Information accompanies this paper on Heredity website (http://www.nature.com/hdy)

# *Supplementary Information*

*Supplementary Methods S1: Modelling direct and indirect genetic effects*

After accounting for the effects of fixed factors and residual autocorrelation, the adjusted mycelium growth rate of a focal genotype *i* growing on the $p^{th}$ plate in stack $s$ was:

$$z_{i_p s} = D_{i_p} + \sum_{k=p-3}^{p-1} f_{j_k} N_{j_k}^{below} + \sum_{k=p+1}^{p+3} f_{j_k} N_{j_k}^{above} + \sum_{k=p-3}^{p-1} f_{j_k} I_{i_p j_k}^{below} + \sum_{k=p+1}^{p+3} f_{j_k} I_{i_p j_k}^{above} + a_s + \varepsilon_{i_p s} \qquad (1),$$

where $z_{i_p s}$ is the growth rate of the focal genotype $i$ and $D_{i_p}$ is its direct genetic effect, $j_k$ is the neighbour genotype growing at position $k$ within the same stack and its main (respectively G x G) indirect genetic effect with the neighbour genotype is $N_{j_k}^{below}$ or $N_{j_k}^{above}$ (respectively $I_{i_p j_k}^{below}$ or $I_{i_p j_k}^{above}$) depending on whether it is placed below or above the focal genotype. $f_{j_k}$ is the intensity of interaction factor (see below), $a_s$ is a random stack effect and $\varepsilon_{i_p s}$ is the residual error term (see Figure S1 below). We did not assume the interactions between two genotypes to be reciprocal. In other words, the effect of a first genotype on the growth rate of a second genotype growing one plate below could differ from the effect of the second genotype on the growth rate of the first genotype (i.e. $I_{i_p j_{p-1}}^{below}$ and $I_{i_{p-1} j_p}^{above}$ were fitted independently).

For model with no genetic covariance between DGEs and main IGEs, we also tested for directionality of IGEs by comparing models where IGEs were similar or different for a given genotype placed above or below the focal plate (for main IGEs: $\boldsymbol{u_n} = \begin{pmatrix} \boldsymbol{u_{n\ above}} \\ \boldsymbol{u_{n\ below}} \end{pmatrix}$ with $V[\boldsymbol{u_{n\ below}}] = \sigma^2_{n\ below}\ I_{n\ below}$ and $V[\boldsymbol{u_{n\ above}}] = \sigma^2_{n\ above}\ I_{n\ above}$ and for G x G IGEs:$\boldsymbol{u_i} = \begin{pmatrix} \boldsymbol{u_{i\ above}} \\ \boldsymbol{u_{i\ below}} \end{pmatrix}$ with $V[\boldsymbol{u_{i\ below}}] = \sigma^2_{i\ below}\ I_{i\ below}$ and $V[\boldsymbol{u_{i\ above}}] = \sigma^2_{I\ above}\ I_{i\ above}$, see Table S2 for the dimensions of the different identity matrices).

To determine the distance over which IGEs occurred, we compared a model where the intensity of IGEs decreased with the inverse of the distance between the plates of the focal

and neighbour genotypes (intensity of interaction factors: $f_{j_{p-1}} = f_{j_{p+1}} = 1$, $f_{j_{p-2}} = f_{j_{p+2}} = \frac{1}{2}$ and $f_{j_{p-3}} = f_{j_{p+3}} = \frac{1}{3}$, Costa e Silva and Kerr, 2013, "distance effect" in Table S2) to a model where IGEs only occur with neighbour genotypes one plate away from the focal genotype (intensity of interaction factors: $f_{j_{p-1}} = f_{j_{p+1}} = 1$ and $f_{j_{p-2}} = f_{j_{p+2}} = f_{j_{p-3}} = f_{j_{p+3}} = 0$, "no distance effect" in Table S2).

To test for differences in IGEs for a given neighbour genotype placed above or below a focal plate (i.e. directionality of IGEs), we compared the model in equation 1 to a model in which a given neighbour genotype had the same IGE when placed above or below the focal genotype (i.e. $N_{j_k}^{below} = N_{j_k}^{above}$ and $I_{i_p j_k}^{below} = I_{i_p j_k}^{above}$).

For datasets 1 and 2, the adjusted growth rate could be respectively modelled as:

$$z_{i_p s} = D_{i_p} + f_{j_{p-1}} N_{j_{p-1}}^{below} + f_{j_{p+1}} N_{j_{p+1}}^{above} + f_{j_{p-1}} I_{i_p j_{p-1}}^{below} + f_{j_{p+1}} I_{i_p j_{p+1}}^{above} + a_s + \varepsilon_{ip} \quad (2)$$

and

$$z_{i_p s} = D_{i_p} + \sum_{k=p-2}^{p-1} f_{j_k} N_{j_k}^{below} + \sum_{k=p+1}^{p+2} f_{j_k} N_{j_k}^{above} + \sum_{k=p-2}^{p-1} f_{j_k} I_{i_p j_k}^{below} + \sum_{k=p+1}^{p+2} f_{j_k} I_{i_p j_k}^{above} + a_s + \varepsilon_{i_p s} \quad (3).$$

See main text and text above for details.

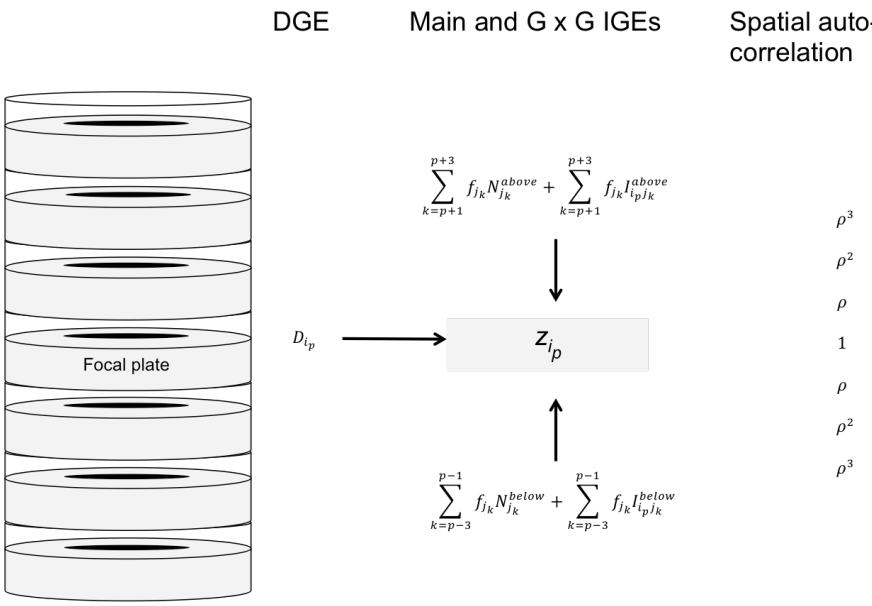


**Figure S1** Schematic representation of the different genetic effects fitted (the genetic covariance between $D_{i_p}$ and $N_j$ has been omitted for clarity). $D_{i_p}$ is the DGE of the focal genotype, the different $N_j$ and $I_{i_p j}$ respectively correspond to the main and G x G IGEs of the different neighbour genotypes indexed according to their position relative to the focal genotype at the $p^{\text{th}}$ position within the stack. See text above for details.

*Supplementary Methods S2: Potential origin of main IGEs*

Let's assume that IGEs are proportional to the genotypic growth rate of the neighbour genotype (e.g. the production of a signalling molecule is proportional to growth rate). We can imagine two scenarios that both predict strong main IGEs. In the first scenario, imagine that the growth rate of a focal genotype is altered independently of its own genotypic growth rate value because some genotypes inhibit or stimulate all their neighbours similarly (i.e. there would be universal inhibitor/stimulator genotypes) by depleting a common resource such as oxygen. Under this scenario, we expect to detect a main IGEs and a correlation between DGEs and main IGEs.

In the second scenario, imagine the growth rate of a focal genotype is altered in proportion to the difference between its own genotypic value for growth rate and the genotypic value of its neighbour. Now, a focal strain with an average growth rate would grow

slower when placed with a fast growing neighbour genotype, but would grow faster when placed with a slow growing neighbour genotype. If the IGE is directly proportional to the difference of genotypic values between the focal strain and its neighbour, we have the following expression:

$$\boldsymbol{z_{ijk} = \mu + D_i + \alpha(D_i - D_j) + \varepsilon_{ijk}} \quad (4a),$$

where $\boldsymbol{z_{ijk}}$, is the growth rate of a focal strain of genotype $\boldsymbol{i}$ with genotypic value, $\boldsymbol{D_i}$, placed close to a neighbour strain $\boldsymbol{j}$ with genotypic value $D_j$. $\boldsymbol{\alpha}$ is the interaction coefficient which relates the observed IGEs to the difference in DGEs between focal and neighbour strains. $\boldsymbol{\varepsilon_{ijk}}$ is the measurement error. Equation 3a can be rewritten as:

$$\boldsymbol{z_{ijk} = \mu + D'_i + D'_j + \varepsilon_{ijk}} \quad (4b),$$

where $\boldsymbol{D'_i}$ is the DGE of focal genotype $\boldsymbol{i}$ (with $\boldsymbol{D'_i = (1 + \alpha)D_i}$) and $\boldsymbol{D'_j}$ represents the main IGE of neighbour genotype $\boldsymbol{j}$ (with $\boldsymbol{D'_j = \alpha D_j}$). In other words, the average growth rate of a focal strain across all neighbours would depend on $\boldsymbol{D_i}$ and $\boldsymbol{\alpha}$, while the effect average effect of a genotype on the growth of its neighbours would depend on $\boldsymbol{D_j}$ and $\boldsymbol{\alpha}$. Although the IGEs biologically represent a G x G IGEs (as the effect of a neighbour genotype depends on the genotype of the focal genotype), it represents a main IGE statistically. Hence, we expect to detect a main IGEs and no G x G IGEs under this scenario.

*Supplementary Methods S3: Power analyses*

Relative importance of main and G x G IGEs

As the number of levels available to estimate main and G x G IGEs decreased in dataset 3 compared to datasets 1 and 2 (Table S2), we estimated our power of detecting effects, given that they exist, using simulation-based power analyses based on our experimental design (Johnson *et al.*, 2015). We used the estimates from the model with lowest AICc for each variance component. In the first power analysis, we simulated datasets with intensity of interaction factors with neighbour genotypes that were proportional to the distance between

focal and neighbour genotypes (see above). In the second power analysis, we simulated datasets with different $\sigma^2_{n_{p\pm1}}$ (variance of main IGEs due to genotypes one plate way from the focal genotype). The proportion of variance explained by $\sigma^2_{n_{p\pm1}}$ ranged from 0 to 17% ($\sigma_{n_{p\pm1}} =$ 0.001, 0.01, 0.02, 0.025, 0.03, 0.035, 0.04, 0.045, 0.05, 0.055, 0.06, 0.065, 0.075, 0.085, 0.1, 0.125, 0.15, 0.2, respectively). In the third power analysis, we simulated datasets with different $\sigma^2_{n_{p\pm1}}$ (variance of main IGEs due to genotypes one plate way from the focal genotype) and different $\sigma_{dn_{p\pm1}}$ (covariance between the colony diameter of a focal genotype and its inhibition effect as a neighbour one plate away from a focal genotype). The proportion of variance explained by $\sigma^2_{n_{p\pm1}}$ ranged from 0 to 17% ( $\sigma_{n_{p\pm1}} =$ 0.01,0.025,0.05,0.06,0.07,0.075,0.08,0.09,0.1,0.125, respectively), while the values of correlation ( $\frac{\sigma_{dn_{p\pm1}}}{\sigma^2_d\sigma^2_{n_{p\pm1}}}$ ) ranged between 0.01 and 0.9 ( $\rho_{dn_{p\pm1}} =$ 0.0001,0.005,0.01,0.05,0.1,0.5,0.75,0.9). We simulated independently 1000 datasets for distance-dependent intensity of interaction factor, for each value of $\sigma^2_{n_{p\pm1}}$ and for each combination of $\sigma^2_{n_{p\pm1}}$ and $\sigma_{dn_{p\pm1}}$. We analysed each dataset using either the original model used for the simulations or an alternative model without the tested effect. Power was estimated as the proportion of the 1000 datasets in which the model used for the simulations for amongst the best model (i.e. $\mathrm{AICc(reduced\ model)} - \mathrm{AIC(original\ model)} > -2$. We used an arbitrary threshold of a power of 80% for the analyses (Johnson *et al.*, 2015).

*Supplementary Results S1*

Relative importance of main and G x G IGEs

For datasets 1, 2 and 3, models including the effects of DGEs and G x G IGEs were strongly supported ($\Delta AIC > 2$ for models without these effects, Tables S3, S4 and S5). In contrast, models including additive IGEs were not supported in the analyses of datasets 1 and 2

($\Delta AIC > 2$ for models with these effects, Tables S3 and S4), and were weakly supported in the analysis of dataset 3 ($\Delta AIC = 1.16$ for a model including directional additive IGEs, Table S5). Models including different vs. the same effects when the neighbour strain was above or below the focal strain (directionality or non-directionally of the G x G IGEs) had different degrees of support depending on the datasets. Models with directional IGEs were weakly supported in dataset 1 ($\Delta AIC = 0.82$ for a model including these directional effects, Table S3), strongly supported in dataset 2 ($\Delta AIC > 2$ for models with non-directional IGEs, Table S4), and were not supported in dataset 3 ($\Delta AIC = 3.98$ for models with directional IGEs, Table S4). G x G IGEs with strains two plates away from the focal strain could only be investigated using datasets 2 and 3. Models including such G xG IGEs were highly supported in dataset 2 ($\Delta AIC = 6.40$ for a model excluding this effect, Table S4), but were weakly supported in dataset 3 ($\Delta AIC = 1.89$ for a model including this effect, Table S5).

**Table S1 List of the 41 strains used for the experiment.**

**Table S2 Number of levels available to estimate DGEs ($u_d$), main IGEs ($u_n$, $u_{n\,below}$, $u_{n\,above}$), and G x G IGEs ($u_i$, $u_{i\,below}$, $u_{i\,above}$) in each of the three datasets analysed.**

**Table S3A Model selection of focal colony diameter as a function of DGEs, main and G x G IGEs for dataset 3.**

**Table S3B Incremental Wald test of the G x G IGE model including two fixed effects (agar status focal and agar status neighbour) for dataset 3.**

**Table S4A Model selection of focal colony diameter as a function of DGEs, main and G x G IGEs for dataset 1.**

**Table S4B Incremental Wald test of the G x G IGE model including two fixed effects (agar status focal and agar status neighbour) for dataset 1.**

**Table S5A Model selection of focal colony diameter as a function of DGEs, main and G x G IGEs for dataset 2.**

**Table S5B Incremental Wald test of the G x G IGE model including two fixed effects (agar status focal and agar status neighbour) for dataset 2.**

**Table S6 Estimates of the variance components fitted for DGEs, G x G IGEs and spatially correlated environmental effects (dataset 3).**

# *References*

Costa e Silva J, Kerr RJ (2013). Accounting for competition in genetic analysis, with particular emphasis on forest genetic trials. *Tree Genet genomes* **9**: 1–17.

Johnson PCD, Barry SJE, Ferguson HM, Müller P (2015). Power analysis for generalized linear mixed models in ecology and evolution. *Methods Ecol Evol* **6**: 133–142.

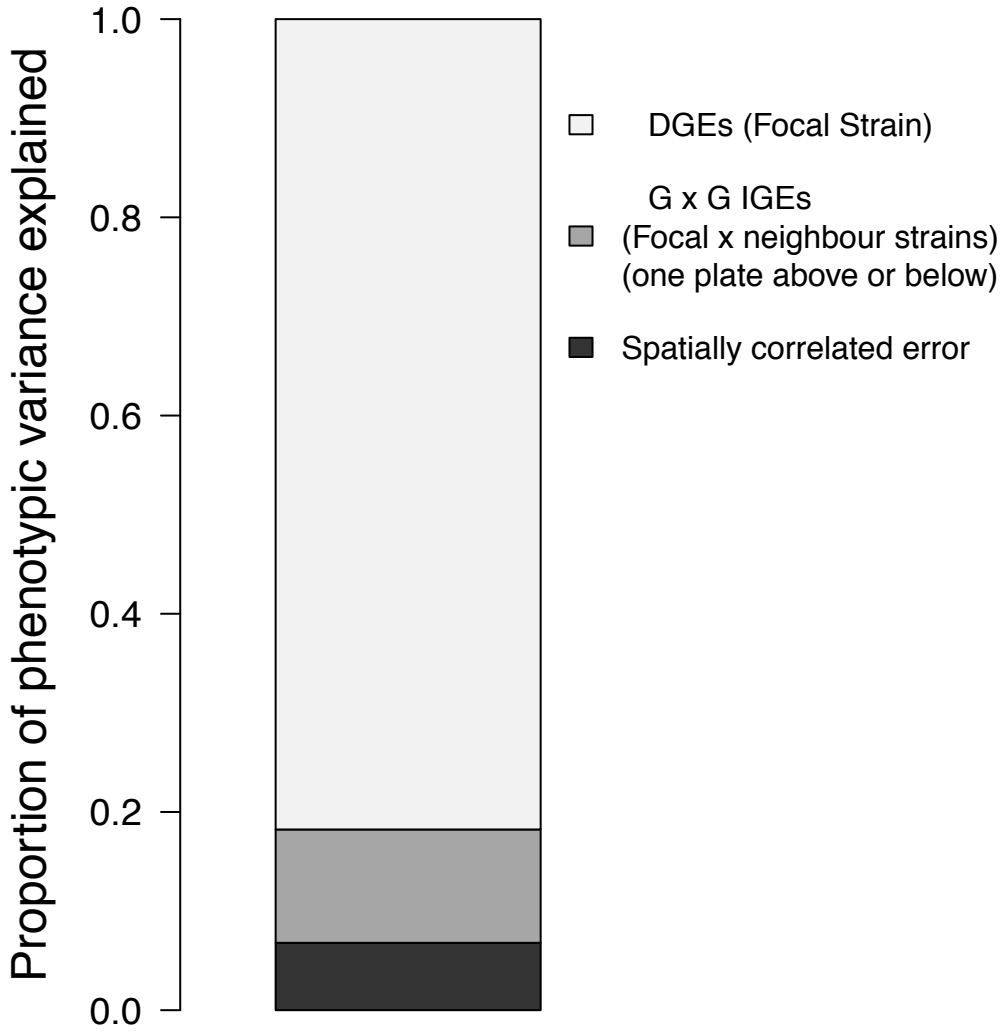


**Figure S2** Proportion of variance in growth rate explained by direct genetic effects (DGEs = 81.8%, focal strain), genotype by genotype indirect genetic effects (G x G IGEs between focal and neighbour strains one plate apart = 11.4%) and environmental effects (spatially correlated error = 6.8%). Models including G x G IGEs between focal and neighbour strains more than one plate away or main IGEs had low support (see main text).

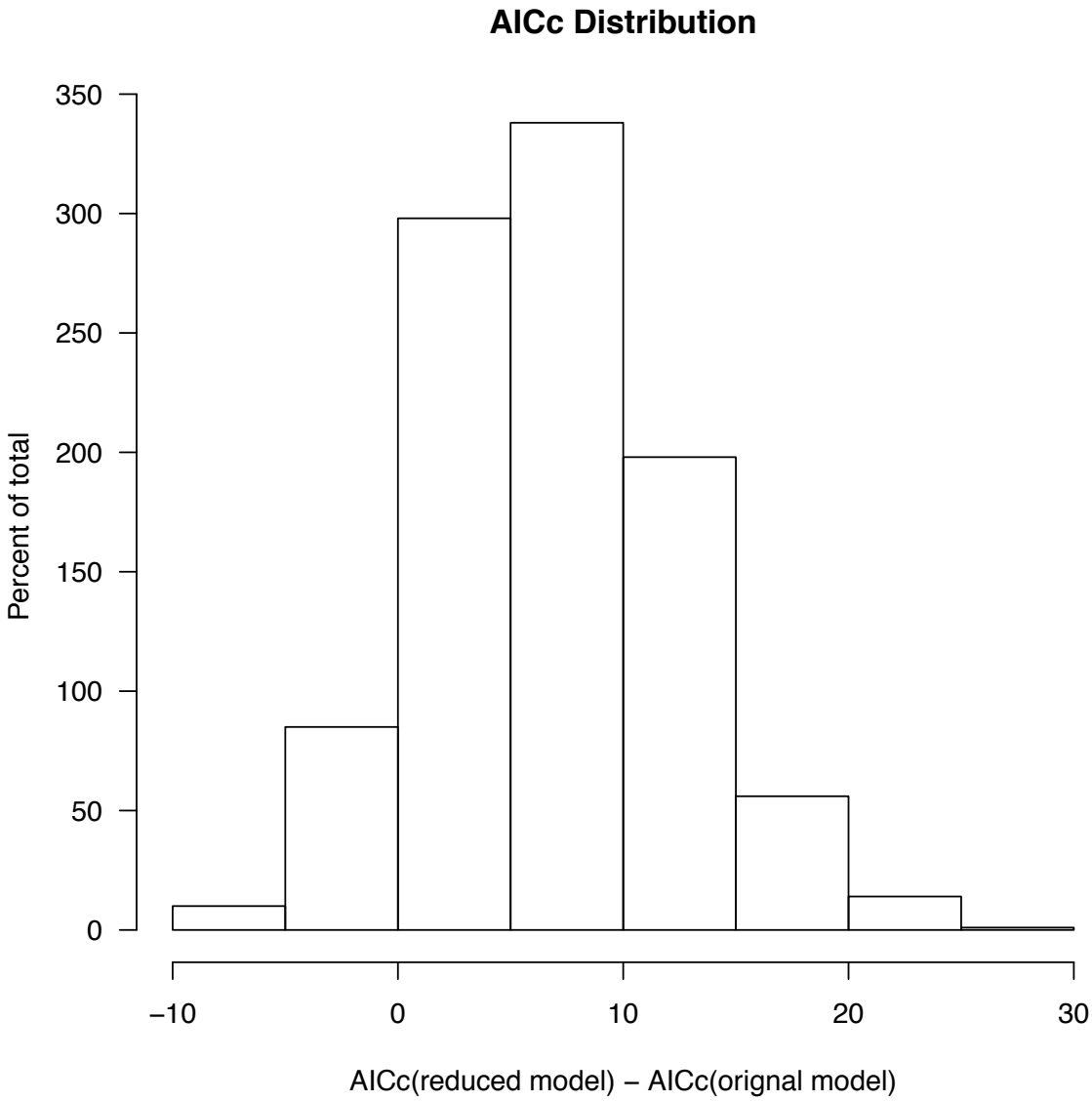


**Figure S3** Distribution of AICc differences between the reduced model and the original model used for the simulation. The original model was among the best models in 97% of the simulations (n = 1000 simulated datasets, see Supplementary Methods S2).

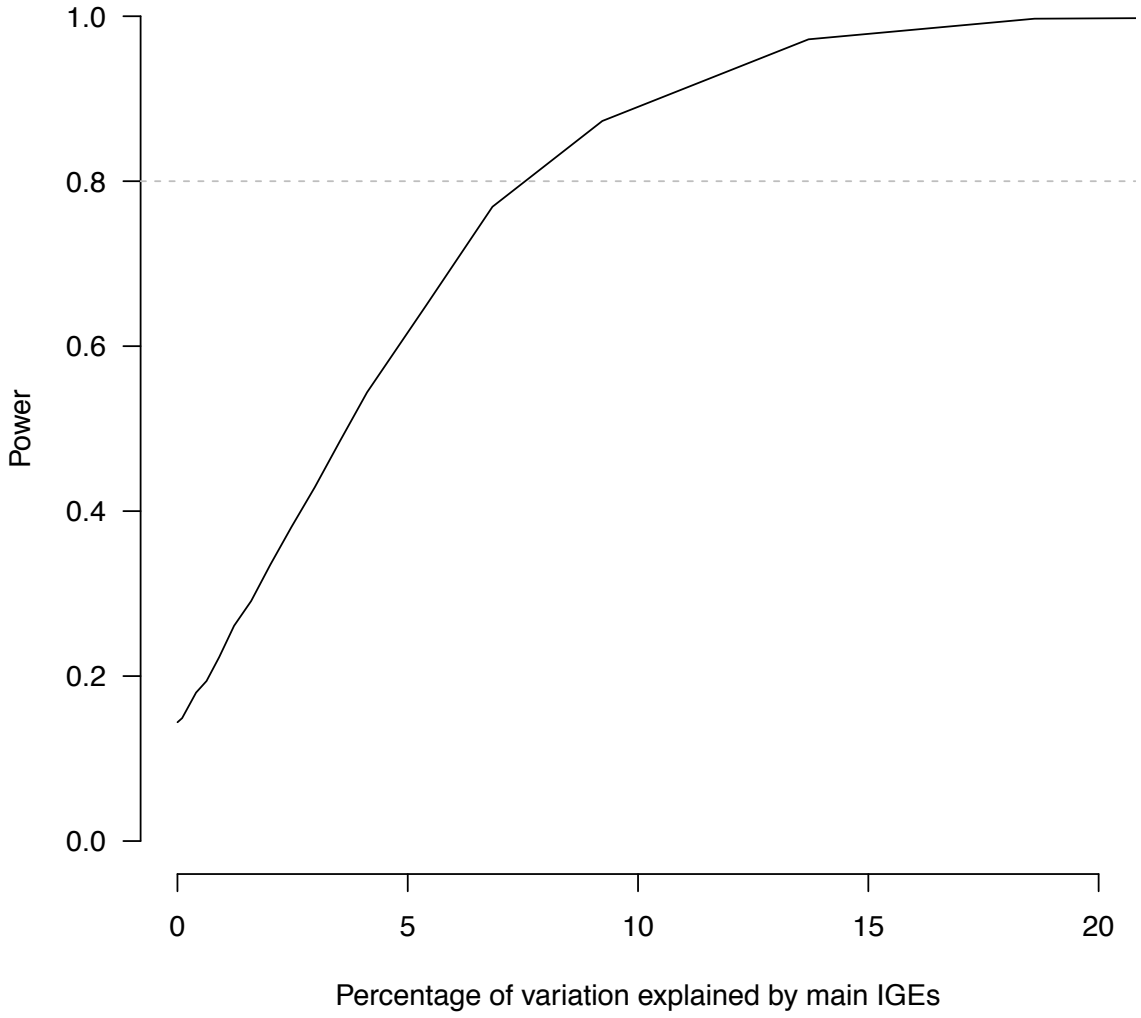


**Figure S4** Power as a function of the proportion of the total phenotypic variance explained by the variance in main IGEs. Power was estimated based on 1000 simulated datasets for each value of $\sigma^2_{N_{p\pm1}}$ (see Supplementary Methods S2). The dashed line represents an arbitrary threshold power of 80%.

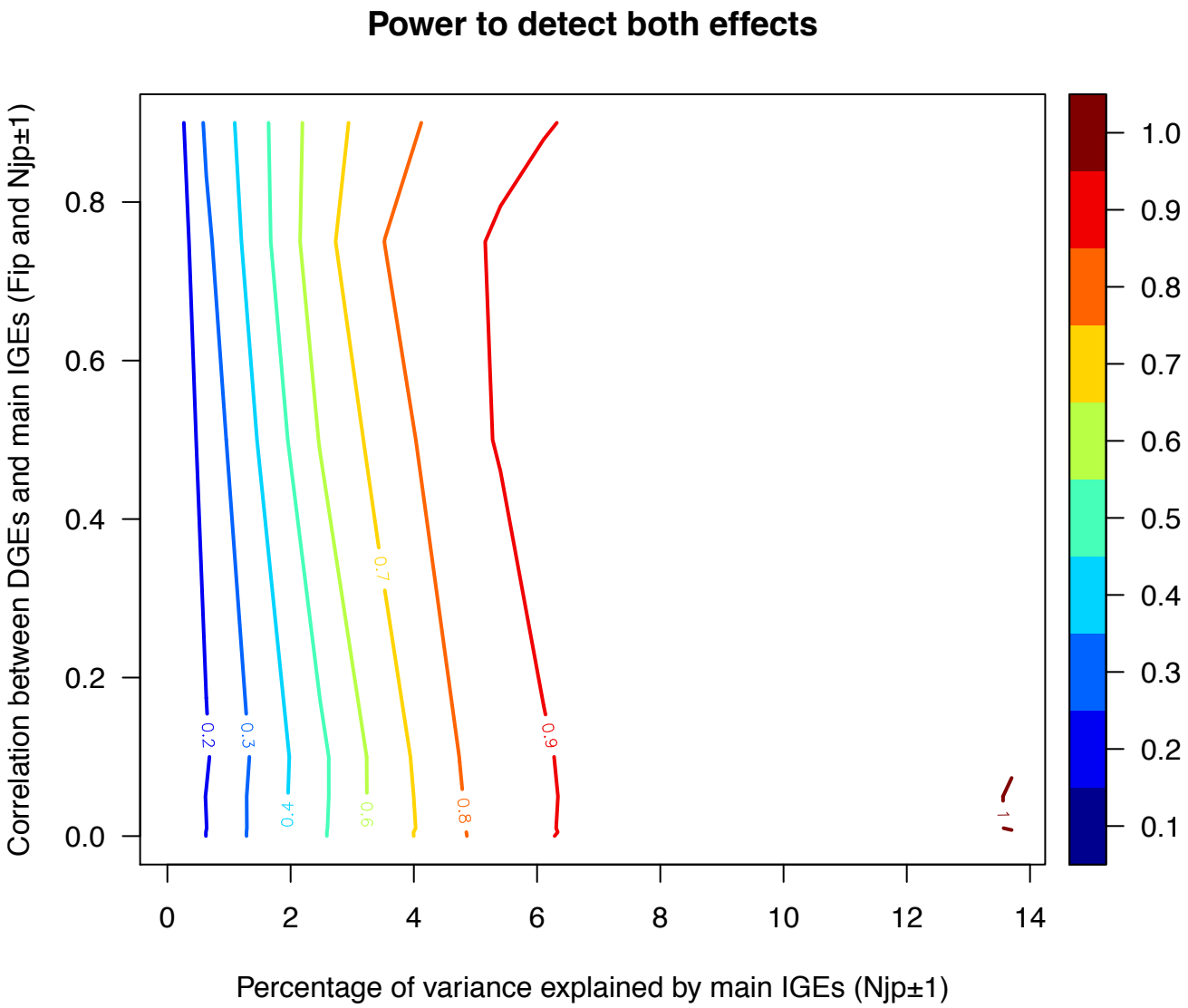


**Figure S5** Power as a function of the proportion of the total phenotypic variance explained by the variance in main IGEs and by the genetic correlation between DGEs and these main IGEs. Power was estimated based on 100 simulated datasets for each value of $cor_{F,N_{p\pm1}}$ (see Supplementary Methods S2). The arbitrary threshold power of 80% is represented in orange.

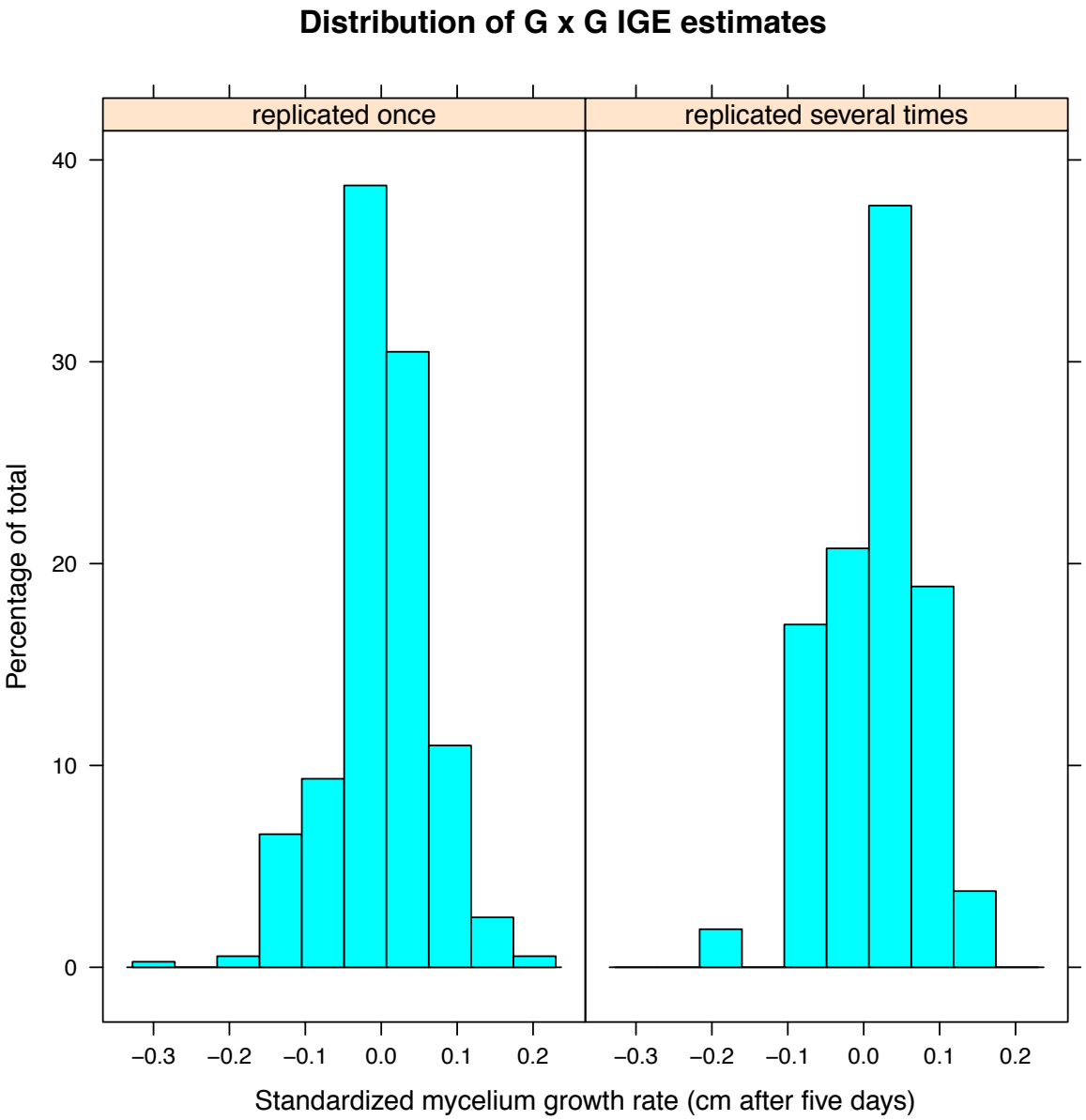


**Figure S6** Distribution of G x G IGE estimates for pairs of strains replicated once or several times. The variance between pairs replicated only once does not seem greater than the variance between pair replicated several times.

**Table S1 List of the 41 strains used for the experiment.**

| Isolate # * | Stock Center | Alternative Isolate # ** | Origin | City | Location (England County/Country) | Heterokaryon Compatibility Group | Isolation Date | Genotyping information available |
|---|---|---|---|---|---|---|---|---|
| WG638w*** | UO | - | Lab | - | - | JC257 | - | 0 |
| 26161 | IBT | 28 | Wild | Birmingham | Birmingham | A | mar-62 | 0 |
| 26166 | IBT | 51 | Wild | Durham | Durham | G | 1962 | 0 |
| A4 | FGSC | FGSC4 | Wild | Glasgow? | Glasgow? | GL | Unknown | 1 |
| A92 | FGSC | 26 | Wild | Birmingham | Birmingham | B | 1961 | 0 |
| A96 | FGSC | 44 | Wild | Beamish | Durham | A | Unknown | 0 |
| A991 | FGSC | 65 | Wild | Birmingham | Birmingham | A | oct-66 | 1 |
| A992 | FGSC | 1 | Wild | Birmingham | Birmingham | B | 1954 | 1 |
| A994 | FGSC | 34 | Wild | Edgebaston | Birmingham | D | apr-62 | 1 |
| A995 | FGSC | 43 | Wild | Beamish | Durham | E | jun-62 | 1 |
| A996 | FGSC | 108 | Wild | Kent | Kent | F | nov-62 | 1 |
| A998 | FGSC | 109 | Wild | Kent | Kent | H | nov-62 | 1 |
| A999 | FGSC | 66 | Wild | Edgebaston | Birmingham | I | nov-62 | 1 |
| A1000 | FGSC | 67 | Wild | Birmingham | Birmingham | J | nov-62 | 1 |
| A1001 | FGSC | 68 | Wild | Birmingham | Birmingham | K | nov-62 | 1 |
| A1002 | FGSC | 80 | Wild | Pembroke | Pembrokeshire | L | nov-62 | 1 |
| A1003 | FGSC | 85 | Wild | Pembroke | Pembrokeshire | M | nov-62 | 1 |
| A1004 | FGSC | 89 | Wild | Cambridgeshir | Cambridgeshire | N | nov-62 | 1 |
| A1005 | FGSC | 106 | Wild | Warwick | Warwickshire | Q | nov-62 | 1 |
| A1006 | FGSC | 99 | Wild | Portsmouth | Hampshire | R | nov-62 | 1 |
| A1007 | FGSC | 114 | Wild | Pembrokeshir | Pembrokeshire | U | nov-62 | 1 |
| A1008 | FGSC | 154 | Wild | Devon | Devon | V | jun-63 | 1 |
| JC257**** | WG | 257 | Wild | Unknown | Hungary | JC257 | 1981 | 0 |
| JC257w*** | WG | 257 | Lab | - | - | JC257 | - | 0 |
| S1 | WG | - | MA | - | - | JC258 | - | 0 |
| S3 | WG | - | MA | - | - | JC259 | - | 0 |
| S5 | WG | - | MA | - | - | JC260 | - | 0 |
| S6 | WG | - | MA | - | - | JC261 | - | 0 |

| | | | | | | | | |
|---|---|---|---|---|---|---|---|---|
| S7 | WG | - | MA | - | - | JC261 | - | 0 |
| S8 | WG | - | MA | - | - | JC261 | - | 0 |
| S9 | WG | - | MA | - | - | JC262 | - | 0 |
| S10 | WG | - | MA | - | - | JC263 | - | 0 |
| S11 | WG | - | MA | - | - | JC264 | - | 0 |
| S15 | WG | - | MA | - | - | JC265 | - | 0 |
| S16 | WG | - | MA | - | - | JC266 | - | 0 |
| S17 | WG | - | MA | - | - | JC267 | - | 0 |
| S18 | WG | - | MA | - | - | JC268 | - | 0 |
| S19 | WG | - | MA | - | - | JC269 | - | 0 |
| S20 | WG | - | MA | - | - | JC270 | - | 0 |
| S21 | WG | - | MA | - | - | JC271 | - | 0 |
| S22 | WG | - | MA | - | - | JC272 | - | 0 |

* Genotype number as provided by the stock center (UO: University of Ottawa, Ottawa, Canada; IBT: IBT Culture Collection of Fungi, Technical University of Denmark, Lyngby, Denmark; FGSC: Fungal Genetic Stock Center, University of Missouri, Kansas City, Missouri, USA; WG: University of Wageningen, Wageningen University, Wageningen, The Netherlands)

** Collection number used in seminal papers [1–4]

*** A4, the "Glasgow wild-type" strain used widely in research, is of unknown geographical origin [5].

*** Mutant with white conidiospores (spontaneous for JC257w, UV-induced for WG638w)

**** Ancestor used for the mutation accumulation experiment originally sampled in Hungary. MA lines and JC257w differ from their ancestor by relatively few mutations [6].

References:


1 Coenen, A., Croft, J. H., Slakhorst, M., Debets, F. & Hoekstra, R. 1996 Mitochondrial inheritance in Aspergillus nidulans. *Genet. Res.* **67**, 93–100.

2 Grindle, M. 1963 Heteorokaryon compatibility of closely related wild isolates of *Aspergillus nidulans*. *Heredity (Edinb).* **18**, 397–405.

3 Grindle, M. 1963 Heterokaryon compatibility of unrelated strains of the *Aspergillus nidulans* group. *Heredity (Edinb).* **18**, 191–204.

4 Butcher, A. C. 1968 The relationship between sexual outcrossing and heterokaryon incompatibility in Aspergillus nidulans. *Heredity (Edinb).* **23**, 443–452.

5 Geiser, D. M., Arnold, M. L. & Timberlake, W. E. 1994 Sexual origins of British *Aspergillus nidulans* isolates. *Proc. Natl. Acad. Sci. U. S. A.* **91**, 2349–2352.

6 Bruggeman, J., Debets, a. J. M., Wijngaarden, P. J., DeVisser, J. a G. M. & Hoekstra, R. F. 2003 Sex slows down the accumulation of deleterious mutations in the homothallic fungus Aspergillus nidulans. Genetics 164, 479–485.

**Table S2 Number of levels available to estimate DGEs ($u_d$), main IGEs ($u_n$, $u_{n\ below}$, $u_{n\ above}$), and G x G IGEs ($u_i$, $u_{i\ below}$, $u_{i\ above}$) in each of the three datasets analysed.**
Main IGEs and G x G IGEs could vary depending on the position of the neighbour genotype relative to the focal genotypes (directional) or not (non-directional).
IGEs could occur with neighbours one plate above or below the focal plate (no distance effect, datasets 1, 2 and 3) or with neighbours one and two plates away (dataset 2) or one, two and three plates away (dataset 3) from the focal. Numbers between parentheses indicate the number of levels estimated with two independent replictates or more (most focal genotype/neighbour genotype combinations appear only a few time)

| | DGEs | Main IGEs | | G x G IGEs | |
|---|---|---|---|---|---|
| **Dataset analyzed** | **Dimension of $u_d$** | **Dimension of $u_{n\ below}$ / $u_{n\ above}$ (Directionality)** | **Dimension of $u_n$ (No directionality)** | **Dimension of $u_{i\ below}$ / $u_{i\ above}$ (Directionality)** | **Dimension of $u_i$ (No directionality)** |
| dataset 1 | 41 | no distance effect: 41 / 41 | no distance effect: 41 | no distance effect: 275 (26) / 274 (27) | no distance effect: 513 (83) |
| dataset 2 | 41 | no distance effect: 41 / 41<br>distance effect: 41 / 41 | no distance effect: 41<br>distance effect: 41 | no distance effect: 249 (21) / 248 (22)<br>distance effect: 464 (72) / 470 (65) | no distance effect: 470 (64)<br>distance effect: 817 (222) |
| dataset 3 | 41 | no distance effect: 41 / 41<br>distance effect: 41 / 41 | no distance effect: 41<br>distance effect: 41 | no distance effect: 221 (17) / 220 (18)<br>distance effect: 587 (115) / 588 (114) | no distance effect: 417 (53)<br>distance effect: 1000 (327) |

**Table S3A Model selection of focal colony diameter as a function of DGEs, main and G x G IGEs for dataset 3.**

We report the number of fitted parameters (k), logLikelihood compared to the loglikelihood of the best model of 235.18 (ΔLL), difference in corrected Akaike's information criteria compared to the best model (ΔAICc) and model weight (w). All the parameters from the best model are indicated in the first row of the table. For simplicity only the effects different from the best model are shown for the other models (see Figure S1 and methods for details).

| model | directionality | K | ΔLL | ΔAICc | weight | Main IGEs | G x G IGEs |
|---|---|---|---|---|---|---|---|
| G x G IGE model | no | 6 | 0.00 | 0.00 | 0.37 | no (fp-3=fp-2=fp-1=fp+1=fp+2=fp+3=0) | 1 plate away (fp-3=fp-2=fp+2=fp+3=0;fp-1=fp+1=1) |
| full model | no | 7 | 0.00* | 2.12 | 0.13 | 1 plate away (fp-3=fp-2=fp+2=fp+3=0;fp-1=fp+1=1) | |
| full model | no | 7 | 0.00* | 2.12 | 0.13 | 3 plates away (fp-3=fp+3=1/3; fp-2=fp+2=1/2; fp-1=fp+1=1) | |
| G x G IGE model | no | 7 | 0.00* | 2.12 | 0.13 | | |
| G x G IGE model | no | 7 | 0.00* | 2.12 | 0.13 | | |
| G x G IGE model | yes | 7 | 0.93 | 3.98 | 0.05 | | |
| full model | no | 8 | 0.00* | 4.26 | 0.04 | 1 plate away (fp-3=fp-2=fp+2=fp+3=0;fp-1=fp+1=1) | |
| G x G IGE model | yes | 7 | 2.36 | 6.84 | 0.01 | | 2 plates away (fp-3=fp+3=0;fp-2=fp+2=1/2;fp-1=fp+1=1) |
| G x G IGE model | no | 7 | 3.36 | 8.84 | 0.00 | | |
| G x G IGE model | no | 5 | 7.85 | 13.59 | 0.00 | | |

| | | | | | | | |
|---|---|---|---|---|---|---|---|
| G x G IGE model | no | 6 | 8.14 | 16.29 | 0.00 | | 3 plates away (fp-3=fp+3=1/3; fp-2=fp+2=1/2; fp-1=fp+1=1) |
| No IGE model | no | 5 | 11.18 | 20.26 | 0.00 | | no (fp-3=fp-2=fp-1=fp+1=fp+2=fp+3=0) |
| main IGE model | no | 6 | 11.18 | 22.36 | 0.00 | 1 plate away (fp-3=fp-2=fp+2=fp+3=0;fp-1=fp+1=1) | no (fp-3=fp-2=fp-1=fp+1=fp+2=fp+3=0) |
| main IGE model | no | 6 | 11.18 | 22.36 | 0.00 | 3 plates away (fp-3=fp+3=1/3; fp-2=fp+2=1/2; fp-1=fp+1=1) | |
| main IGE model | yes | 7 | 10.89 | 23.91 | 0.00 | 1 plate away (fp-3=fp-2=fp+2=fp+3=0;fp-1=fp+1=1) | |
| G x G IGE model | no | 5 | 21.66 | 41.21 | 0.00 | | |

* Some models converged with a random effect variance close to zero and had the same log-likelihood as the model with lowest AICc.

**Table S3B Incremental Wald test of the G x G IGE model including two fixed effects (agar status focal and agar status neighbour) for dataset 3.**

| | Df | Denominator Df | F | Pr(Chisq) | |
|---|---|---|---|---|---|
| (Intercept) | 1 | 47.50 | 9316.00 | 3.72E-56 | *** |
| Agar status focal | 1 | 190.70 | 24.27 | 1.81E-06 | *** |
| Agar status neighbour | 1 | 195.40 | 1.04 | 3.10E-01 | |

This model corresponds to model m25 in the Dryad script. Denominator degrees of freedor computed using Kenward & Rogers formula (Kenward and Roger, 1997).

References:

Kenward, M. G., & Roger, J. H. (1997). Small sample inference for fixed effects from restricted maximum likelihood. *Biometrics*, 983-997.

| Correlation DGEs/Main IGEs | Fixed effect | Stack effect | Spatially correlated error | Spatially uncorrelated error | corresponding model on Dryad |
|---|---|---|---|---|---|
| no | Agar status focal | no | yes | no | m0 |
| | | | | | m3 |
| | | | | | m4 |
| | | yes | | | m22 |
| | | | | yes | m23 |
| | | | | | m9 |
| yes | | | | | m17 |
| | | | | | m10 |
| | Agar status focal<br>Agar status neighbour | | | | m25 |
| | No agar status focal | | | | m24 |

| | | |
|---|---|---|
| | | m2 |
| | | m11 |
| | | m12 |
| | | m14 |
| | | m13 |
| | no | m21 |

**Table S4A Model selection of focal colony diameter as a function of DGEs, main and G x G IGEs for dataset 1.**

We report the number of fitted parameters (k), logLikelihood compared to the loglikelihood of the best model of 305.24 (ΔLL), difference in corrected Akaike's information criteria compared to the best model (ΔAICc) and model weight (w). All the parameters from the best model are indicated in the first row of the table. For simplicity only the effects different from the best model are shown for the other models (see Figure S1 and methods for details).

| model | directionality | K | ΔLL | ΔAICc | weight | Main IGEs | G x G IGEs | Correlation DGEs/Main IGEs |
|---|---|---|---|---|---|---|---|---|
| G x G IGE model | no | 7 | 0.00 | 0.00 | 0.32 | no (fp-1=fp+1=0) | 1 plate away (fp-1=fp+1=1) | no |
| No IGE model | no | 6 | 1.71 | 1.33 | 0.17 | | no (fp-1=fp+1=0) | |
| full model | no | 8 | 0.00* | 2.11 | 0.11 | 1 plate away (fp-1=fp+1=1) | | |
| G x G IGE model | no | 8 | 0.00* | 2.11 | 0.11 | | | |
| G x G IGE model | no | 6 | 2.24 | 2.39 | 0.10 | | | |
| G x G IGE model | yes | 8 | 0.66 | 3.42 | 0.06 | | | |
| main IGE model | no | 7 | 1.71 | 3.43 | 0.06 | 1 plate away (fp-1=fp+1=1) | no (fp-1=fp+1=0) | |
| full model | no | 9 | 0.00* | 4.23 | 0.04 | | | yes |
| main IGE model | yes | 8 | 1.54 | 5.19 | 0.02 | 1 plate away (fp-1=fp+1=1) | no (fp-1=fp+1=0) | |
| full model | yes | 10 | 0.62 | 7.62 | 0.01 | 1 plate away (fp-1=fp+1=1) | | |
| G x G IGE model | no | 6 | 5.37 | 8.64 | 0.00 | | | |
| G x G IGE model | no | 8 | 3.74 | 9.59 | 0.00 | | | |
| G x G IGE model | no | 5 | 33.96 | 63.75 | 0.00 | | | |

* Some models converged with a random effect variance close to zero and had the same log-likelihood as the model with lowest AICc.

**Table S4B Incremental Wald test of the G x G IGE model including two fixed effects (agar status focal and agar status neighbour) for dataset 1.**

| | Df | Denominator Df | F | Pr(Chisq) | |
|---|---|---|---|---|---|
| (Intercept) | 1 | 49.2 | 9151 | 1.39E-57 | *** |
| Agar status focal | 1 | 239.6 | 18.98 | 1.96E-05 | *** |
| Agar status neighbour | 1 | 259.8 | 0.42 | 5.19E-01 | |

This model corresponds to model m18 in the Dryad script. Denominator degrees of freedor computed using Kenward & Rogers formula (Kenward and Roger, 1997).

References:

Kenward, M. G., & Roger, J. H. (1997). Small sample inference for fixed effects from restricted maximum likelihood. *Biometrics*, 983-997.

| Fixed effect | Stack effect | Spatially correlated error | Spatially uncorrelated error | corresponding model on Dryad |
|---|---|---|---|---|
| Agar status focal | no | yes | yes | m0 |
| | | | | m7 |
| | | | | m1 |
| | yes | | | m16 |
| | | | no | m21 |
| | | | | m6 |
| | | | | m8 |
| | | | | m13 |
| | | | | m9 |
| | | | | m10 |
| No agar status focal | | | | m17 |
| Agar status focal<br>Agar status neighbour | | | | m18 |
| | | no | | m15 |

**Table S5A Model selection of focal colony diameter as a function of DGEs, main and G x G IGEs for dataset 2.**

We report the number of fitted parameters (k), logLikelihood compared to the loglikelhood of the best model of 277.5 (ΔLL), difference in corrected Akaike's information criteria compared to the best model (ΔAICc) and model weight (w). All the parameters from the best model are indicated in the first row of the table. For simplicity only the effects different from the best model are shown for the other models (see Figure S1 and methods for details).

| model | directionality | K | ΔLL | ΔAICc | weight | Main IGEs |
|---|---|---|---|---|---|---|
| G x G IGE model | yes | 7 | 0.00 | 0.00 | 0.38 | no (fp-2=fp-1=fp+1=fp+2=0) |
| G x G IGE model | yes | 8 | 0.18* | 1.76 | 0.16 | |
| full model | no | 8 | 0.00* | 2.12 | 0.13 | 2 plates away (fp-1=fp+1=1;fp-2=fp+2=1/2) |
| G x G IGE model | no | 8 | 0.00* | 2.14 | 0.13 | |
| G x G IGE model | no | 9 | 0.31* | 3.63 | 0.06 | |
| full model | yes | 9 | 0.08* | 4.10 | 0.05 | 2 plates away (fp-1=fp+1=1;fp-2=fp+2=1/2) |
| G x G IGE model | yes | 7 | 2.26 | | 0.04 | |
| G x G IGE model | no | 6 | 4.09 | 6.07 | 0.02 | |
| G x G IGE model | no | 6 | 5.12 | 8.13 | 0.01 | |
| G x G IGE model | yes | 8 | 3.39 | 8.90 | 0.00 | |
| full model | no | 7 | 5.12 | 10.24 | 0.00 | 1 plate away (fp-1=fp+1=1;fp-2=fp+2=0) |
| full model | no | 8 | 5.12 | 12.36 | 0.00 | 1 plate away (fp-1=fp+1=1;fp-2=fp+2=0) |
| G x G IGE model | yes | 6 | 8.96 | 15.81 | 0.00 | |
| No IGE model | no | 5 | 13.59 | 22.97 | 0.00 | |
| main IGE model | no | 8 | 4.83 | 11.78 | 0.00 | 2 plates away (fp-1=fp+1=1;fp-2=fp+2=1/2) |
| main IGE model | no | 6 | 13.59 | 25.06 | 0.00 | 1 plate away (fp-1=fp+1=1;fp-2=fp+2=0) |

| | | | | | | |
|---|---|---|---|---|---|---|
| main IGE model | yes | 7 | 12.87 | 25.74 | 0.00 | 2 plates away (fp-1=fp+1=1;fp-2=fp+2=1/2) |
| G x G IGE model | yes | 6 | 27.26 | 52.41 | 0.00 | |

* Some models converged with a random effect variance close to zero and had the same log-likelihood as the model with lowest AICc.

**Table S5B Incremental Wald test of the G x G IGE model including two fixed effects (agar status focal and agar status neighbour) for dataset 2.**

| | Df | Denominator Df | F | Pr(Chisq) | |
|---|---|---|---|---|---|
| (Intercept) | 1 | 48.3 | 9324.00 | 6.99E-57 | *** |
| Agar status focal | 1 | 210.7 | 27.19 | 4.40E-07 | *** |
| Agar status neighbour | 1 | 215.5 | 1.20 | 2.74E-01 | |

This model corresponds to model m17 in the Dryad script. Denominator degrees of freedor computed using Kenward & Rogers formula (Kenward and Roger, 1997).

References:

Kenward, M. G., & Roger, J. H. (1997). Small sample inference for fixed effects from restricted maximum likelihood. *Biometrics*, 983-997.

| G x G IGEs | Correlation DGEs/Main IGEs | Fixed effect | Stack effect | Spatially correlated error | Spatially uncorrelated error | corresponding model on Dryad |
|---|---|---|---|---|---|---|
| 2 plates away (fp-1=fp+1=1;fp-2=fp+2=1/2) | no | Agar status focal | no | yes | no | m0 |
| | | | | | yes | m18 |
| | | | | | | m3 |
| | | | yes | | | m15 |
| | yes | | | | | m9 |
| | | | | | | m2 |
| 1 plate away (fp-1=fp+1=1;fp-2=fp+2=0) | | | | | | m5 |
| | | | | | | m1 |
| 1 plate away (fp-1=fp+1=1;fp-2=fp+2=0) | | | | | | m6 |
| | | Agar status focal<br>Agar status neighbour | | | | m17 |
| 1 plate away (fp-1=fp+1=1;fp-2=fp+2=0) | | | | | | m4 |
| 1 plate away (fp-1=fp+1=1;fp-2=fp+2=0) | yes | | | | | m10 |
| | | No agar status focal | | | | m16 |
| | | | | | | m7 |
| no (fp-2=fp-1=fp+1=fp+2=0) | | | | | | m11 |
| no (fp-2=fp-1=fp+1=fp+2=0) | | | | | | m8 |

| | | |
|---|---|---|
| no<br>(fp-2=fp-1=fp+1=fp+2=0) | | m12 |
| | no | m14 |

**Table S6 Estimates of the variance components fitted for DGEs, G x G IGEs and spatially correlated environmental effects (dataset 3).**
**Total phenotypic variance is computed by multiplying GxG IGEs variance by two to account for interactions with neighbours above and below the focal strain.**
**The 95% confidence intervals for the proportion of variance explained by each random effect were computed using the delta method.**

| | | Estimate | SE | Proportion of total phenotypic variance explained | 95% CI of the proportion of total phenotypic variance explained |
|---|---|---|---|---|---|
| **Fixed effects** | **Intercept** | 6.550 | 0.347 | | |
| | **Fallen agar status** | -0.133 | 0.055 | | |
| **Random effects** | **DGE ($\sigma_d^2$)** | 0.161 | 0.037 | 81.77% | 73.9-89.6% |
| | **G x G IGE ($\sigma_i^2$)** | 0.011 | 0.002 | 5.72% | 4.9-17.8% |
| | **Environmental variance ($\sigma_{uncor}^2$)** | 0.013 | 0.004 | 6.80% | 1.9-11.7% |
| | **Spatial auto-correlation ($\rho$)** | 0.917 | 0.054 | | |